Arabian Journal of Chemistry (2017) **10**, S1276–S1283

King Saud University

Arabian Journal of Chemistry

www.ksu.edu.sa
www.sciencedirect.com

ORIGINAL ARTICLE

Corrosion inhibition of type 430 stainless steel in an acidic solution using a synthesized tetra-pyridinium ring-containing compound

A.Y. Obaid, A.A. Ganash, A.H. Qusti, Shabaan A. Elroby, A.A. Hermas *

Chemistry Department, Faculty of Science, King Abdulaziz University, Jeddah, Saudi Arabia
Chemistry Department, Faculty of Science, Beni Suef University, Beni Suef, Egypt

Received 2 October 2012; accepted 15 March 2013
Available online 25 March 2013

KEYWORDS

Adsorption;
Chemisorptions;
Corrosion;
Inhibition

Abstract 1,1′-Bis (1-methyl pyridinium-2-yl)-4,4′-dipyridinium dichloride di-iodide (TPy) and 1,1′-dimethyl-4,4′-dipyridinium di-iodide (DPy) have been synthesized and used as corrosion inhibitors for ferritic type 430 stainless steel in 0.5 M H_2SO_4 solution. Polarization, weight loss and scanning electron microscopic measurements confirm the inhibitive action of these compounds and the increase in inhibition efficiency with an increase in concentration and temperature. The compounds enhance the passivation of the steel by increasing suppression of the critical current. The quantum chemical calculations explain the good adsorption of these compounds on the steel surface and the greater inhibition efficiency for TPy compared with that of DPy inhibitor.

1. Introduction

Stainless steel (SS) is used in various applications such as in the oil and petrochemical industry and for parts in desalination plants. Calcium and magnesium-based deposits in desalination plants face unavoidable problems. Acids used to remove such deposits include HCl, H_2SO_4, and HSO_3NH_2 (sulfamic acid). The application of acid corrosion inhibitors in the treatment of scale parts in multistage flash desalination plants is widely used to prevent or minimize material loss during contact with acid. Organic compounds containing heteroatoms with high electron density such as nitrogen, sulfur, and oxygen, or those containing multiple bonds were found to be efficient acid corrosion inhibitors (Al-Mayouf et al., 1998; Hermas et al., 2004).

The organic molecule inhibits the corrosion through its adsorption on the metallic surface. The chemical composition and structure of the inhibitors, nature of the metallic surface, and the properties of the medium significantly influence on the adsorption of the inhibitor (Bentiss et al., 1999). Surfactants, which consist of one polar group (hydrophilic) and one hydrophobic moiety, act as good corrosion inhibitors (Abdel-Aal et al., 1990; El Achouri et al., 2001a,b; Hermas et al., 2004; Wahdan et al., 2002; Migahed, 2005; Noor, 2009; Popova et al., 2007a,b; Saleh, 2006; Li et al., 2011; Stipa, 2006). Some quaternary ammonium bromides of different

* Corresponding author. Address: Chemistry Department, Faculty of Science, Assiut University, Egypt.
E-mail address: hagag_99@yahoo.com (A.A. Hermas).
Peer review under responsibility of King Saud University.

Production and hosting by Elsevier

http://dx.doi.org/10.1016/j.arabjc.2013.03.008
1878-5352

heterocyclic compounds were used as corrosion inhibitors of mild steel in 1 M HCl and 1 M H_2SO_4 by Popova et al. (2007a,b). Viologens (N,N′-diquaternized-4,4′-dipyridinium salts), which have been employed as herbicides, redox mediators, electrochromic materials, electron-transfer quenchers, and as redox probes in self-assembled monolayers (Stipa, 2006; Ock et al., 2005), could be used as efficient corrosion inhibitors (Aziz et al., 1997; Morad et al., 2008). In this study, a new tetra-quaternized-multi-pyrdinium ring compound has been synthesized and was applied as corrosion inhibitors of ferritic stainless steel in sulfuric acid solution.

Recently, computational chemistry has been widely used to explain the mechanism of corrosion inhibition, such as the ab initio quantum chemistry methods (Zhang et al., 2008; Özcan, 2008; Obot et al., 2009; Gece and Bilgiç, 2010). In this work, the electronic and molecular structure of inhibitors will be investigated using density functional calculations.

2. Experimental methods

2.1. Inhibitors synthesis

First, N-methyl-2-chloro-pyridinium iodide was prepared by mixing 2-chloro-pyridine (5 g) with methyl iodide (3 mL) in ethanol (20 mL) for 3 h. The mixture was cooled and then treated with excess ether. The solid salt was filtered, washed with ether, and then dried at 80 °C for 6 h. A solution of 4,4′-bipyridyl (1.0 g) in methanol (10 mL) was added drop wise to a stirred solution of N-methyl-2-chloro-pyridinium iodide (5 g) in methanol (20 mL) under nitrogen atmosphere. The mixture was refluxed for 2 h. The red solid product of 1,1′-bis (1-methyl pyridinium-2-yl)-4,4′-dipyridinium dichloride di-iodide (TPy) was filtered, washed with acetone and dried at 100 °C for 6 h. 1,1′-dimethyl-4,4′-dipyridinium di-iodide (DPy) was synthesized according to Emara (1991). The DPy has a melting point from 295–8 °C and TPy has above 300 °C, the elemental analyses of these compounds are indicated in Table 1 and Fig. 1 shows the chemical structures.

^{1}HNMR data of TPy: δ = 9.4 (d, 4H), 9.3 (d, 2H), 9.0 (t, 2H), 8.63 (d, 2H), 8.5 (t, 2H), 8.07 (d, 4H), 4.3 (s, 6H, 2 CH_3).

2.2. Materials and methods

A standard corrosion glass cell was used for the polarization measurements. The material of the working electrode is a sheet with an area of 1 cm^2 from ferritic type 430 SS, it was cut from cold rolled annealed sheet (produced by Nilaco, Japan and containing 17–18.5% Cr and < 1500 ppm C). The counter and reference electrodes are platinum sheet and silver–silver chloride (Ag/AgCl, 3 M KCl), respectively. The electrolyte solution was prepared from concentrated analytical reagent H_2SO_4 and bi-distilled water. The inhibitor solution was prepared by dissolving the appropriate weight in 0.5 M H_2SO_4 solution.

Table 1 Elemental analysis (%).

Elements	Dpy		TPy	
	Meas.	Cal.	Meas.	Cal.
C	31.2	32.7	38.0	39.6
H	2.48	3.2	2.07	3.3
N	5.82	6.4	6.2	6.4

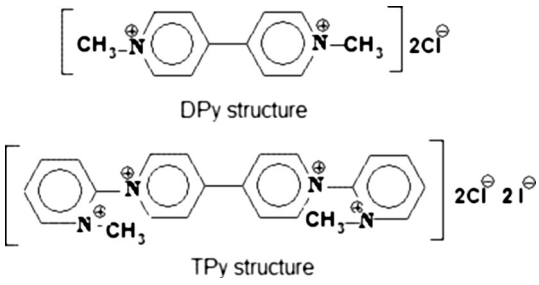

Figure 1 Chemical structure of the inhibitors.

All experiments were conducted thermostatically at a given temperature and in an aerated condition without stirring. Prior to each experiment the working electrode was wet polished with emery papers up to grade 1000, rinsed with bi-distilled water, acetone, bi-distilled water and left in air for 30 min. Then, it was transferred to the glass cell which was filled by 200 ml of the acid solution.

Electrochemical experiments were recorded using a potentiostat of type Autolab PGSTAT30, coupled to a computer equipped with GPES software for potential and polarization measurements. Potentiodynamic measurements were performed with a scan rate of 0.001 V s^{-1}. Scanning electron microscope (SEM) images were obtained by using Joel JSM-6360LVSEM.

2.3. Weight-loss method

Type 430 stainless steel sheets with an area of 10 cm^2, in duplicate, were immersed in aerated 350 mL of 0.5 M H_2SO_4 solution without and with various concentrations of the studied inhibitors for 24 h at 30 °C. The weights of the steel specimens before and after immersion were determined using an analytical balance Mettler AE 166. The corrosion rate in mg dm^{-2} day^{-1} (mdd) was calculated and used in calculation of the inhibition efficiency (IE) according to the equation:

$$IE = \frac{(CR)_1 - (CR)_2}{(CR)_1} \times 100 \quad (1)$$

where $(CR)_1$ and $(CR)_2$ are the corrosion rate of SS in uninhibited and inhibited acid solution, respectively.

2.4. Quantum chemical calculations

The molecular structures of the studied compounds were geometrically optimized using the Density Functional Theory (DFT) method with B3LYP level and 6-31G* basis set, and the Spartan′10 V.1.0.1 program package (Lee et al., 1988). B3LYP, a version of the DFT method that uses Becke's three parameter functional (B3) and includes a mixture of HF with DFT exchange terms associated with the gradient corrected correlation functional of Lee, Yang and Parr (LYP) (Shao et al., 2011), was used in this paper to carry out quantum calculations.

3. Results and discussion

3.1. Polarization measurements

The effects of the synthesized compounds under study on the corrosion and polarization behaviors of the SS were studied

Table 2 Polarization and passivation parameters.

Compd	Concentration	$-E_{cor}$	I_{cor}	b_a	b_c	IE	$-E_{pp}$	I_{crit}	SE
	M	(mV)	(mA cm^{-2})	(mV decade^{-1})		(%)	(mV)	(mA cm^{-2})	(%)
Pure	0	495	3.43	69	164		388	35.5	
DPy	1×10^{-5}	490	3.0	79	173	12.5	388	28.0	21.1
	5×10^{-5}	488	2.26	61	158	34.1	388	29.0	18.3
	1×10^{-4}	477	1.83	78	166	46.6	377	26.3	25.9
	5×10^{-4}	461	0.86	50	169	75.0	372	23.3	34.4
	1×10^{-3}	449	0.48	34	165	86.0	378	19.0	46.5
TPy	1×10^{-5}	494	1.9	70	154	44.6	403	19.9	43.9
	5×10^{-5}	479	1.62	71	149	52.8	388	18.1	49.0
	1×10^{-4}	467	1.01	58	148	70.6	376	16.6	53.2
	5×10^{-4}	452	0.35	31	149	89.8	383	14.1	60.3
	1×10^{-3}	438	0.28	21	149	91.8	378	11.8	66.8

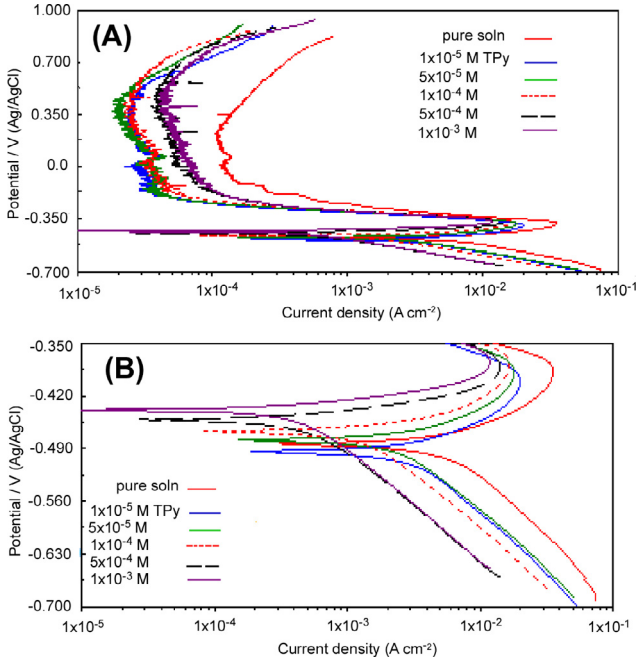

Figure 2 (A) Cathodic–anodic polarization of the SS in 0.5 M H_2SO_4 in the absence and presence of different concentrations of TPy at 30 °C, (B) magnification view of the cathodic–anodic Tafel region.

in 0.5 M H_2SO_4 at 30 °C. Addition of the inhibitor shifted the steel potential (−0.495 V) to the positive side, and this shift in potential increased by increasing inhibitor concentration (−0.449 V and −0.438 V in the case of 1×10^{-3} M of DPy and TPy, respectively), as shown in Table 2. This result indicated that the compounds under study are mainly anodic inhibitors.

Cathodic–anodic polarization of the SS in the absence and the presence of the inhibitor in 0.5 M H_2SO_4 at 30 °C has been performed, as shown in Fig. 2A for the TPy inhibitor. The anodic polarization branch was extended up to the transpassive potential. Complete analysis of the polarization curve, including cathodic–anodic Tafel lines and active–passive range, was done and the parameters are recorded in Table 2 for the two inhibitors. From the corrosion current (i_{cor}), the inhibition efficiency (IE) was calculated using Eq. (2):

Table 3 Weight loss measurement results.

Concen.	DPy		TPy	
M	Corr. rate	IE	Corr. rate	IE
	mdd	(%)	mdd	(%)
0	183		183	
1×10^{-5}	168.4	8.0	136.3	25.5
5×10^{-5}	136.5	25.4	110.6	40.0
1×10^{-4}	107.8	41.1	51.2	72.0
5×10^{-4}	56.7	69.0	23.8	87.0
1×10^{-3}	21.9	88.0	18.2	90.0

$$IE = \frac{i^{\circ}_{cor} - i_{cor}}{i^{\circ}_{cor}} \times 100 \quad (2)$$

where, i°_{cor} is the corrosion current in the absence of the inhibitor. The Tafel line region, as in Fig. 2B, shows that the presence of the TPy compound shifted regularly the cathodic and anodic lines to lower current densities with the inhibitor concentration. A similar behavior was obtained using the DPy compound, indicating that these compounds are mixed type inhibitors with mainly anodic. The TPy inhibitor has more efficient to reduce the corrosion current than the DPy, the difference is clear at the lower concentrations. In the presence of the maximum inhibitor concentration (1 mM), the corrosion current decreased from 3.43 mA cm^{-2} to 0.48 and 0.28 mA cm^{-2} for the DPy and TPy, respectively.

The values of the cathodic slope (b_c) are slightly higher than those of mild steel (Wahdan et al., 2002), primarily the result of the presence of oxide film on the SS surface. The constancy of the b_c values indicates that the mechanism of hydrogen evolution is not changed in the absence and the presence of the inhibitor. The values of b_a decreased at high concentrations of the inhibitor, indicating change in the mechanism of metal dissolution.

The influence of TPy on the passive behavior of SS in H_2SO_4 solution is shown in Fig. 2A. The passivation parameters in the absence and presence of DPy and TPy are recorded in Table 2. The SS showed an active–passive behavior in the studied solutions. Presence of the inhibitor at any concentration did not affect the primary passive potential (E_{pp}) of the SS. However, the current corresponding to E_{pp}, the critical

current density (i_{cit}), decreased gradually with an increase in the inhibitor concentration. i_{crt} is the maximum active anodic current of the SS after which a suppression occurs due to a surface oxide film formation. Presence of the inhibitor was found to decrease i_{crt}, facilitating oxide film formation, which is reflected in a more stable passive range and a lower passive current (lower oxide dissolution), as shown in Fig. 2B. Thus, suppression efficiency (SE) of the inhibitor is significant and could be obtained using Eq. (1) after replacement by i_{crt}. The SE of TPy is higher than that of DPy within the studied inhibitor concentration range, and is 46.5% and 66.8% in the presence of the maximum inhibitor concentration (1 mM) of DPy and TPy, respectively.

3.2. Weight loss measurements

Weight loss measurements of the SS in 0.5 M H_2SO_4 in the absence and the presence of different concentrations of the studied inhibitors were carried out at 30 °C and the results are reported in Table 3. As shown from the results, the corrosion rate of the SS decreased in the presence of the additives and the inhibition efficiency increased with an increase in the concentration of the inhibitor. The TPy compound provides greater inhibition efficiencies than those of DPy within the concentration range under study. The values of inhibition efficiencies calculated from the weight loss method are in good agreement with those calculated from the corrosion current by the polarization method.

3.3. Surface investigation

The SEM images of the SS samples after 12 h immersion in 0.5 M H_2SO_4 in the absence and the presence of 1 mM of the inhibitors under study are shown in Fig. 3. In the pure acid solution the steel suffered from general corrosion as shown in Fig. 3A, where highly attack on the entire surface is observed. The presence of the inhibitor almost prevented the corrosion; in case of the DPy inhibitor very slight attack appears in the medal of the image (Fig. 3B). In case of the TPy inhibitor the image (Fig. 3C) is free from any attack and the polish scratch of the sample is still appearing. These results confirm the polarization and weight loss methods.

3.4. Adsorption isotherm

The organic compounds inhibit the corrosion through its surface adsorption on the metal surface. The fraction of surface coverage (θ) by inhibitor molecules can be calculated from the equation:

$$\theta = \left[1 - \left(\frac{i_{corr}}{i^{\circ}_{corr}}\right)\right] \quad (3)$$

θ is subjected to various adsorption isotherms to find the most suitable adsorption isotherm(s). The inhibitors used in this study are found to fit Langmuir isotherm for monolayer chemisorptions where θ and C (inhibitor's concentration in the bulk of the solution) are related to each other via the equation:

$$\theta = \frac{KC}{(1 + KC)} \quad (4)$$

Rearrangement gives:

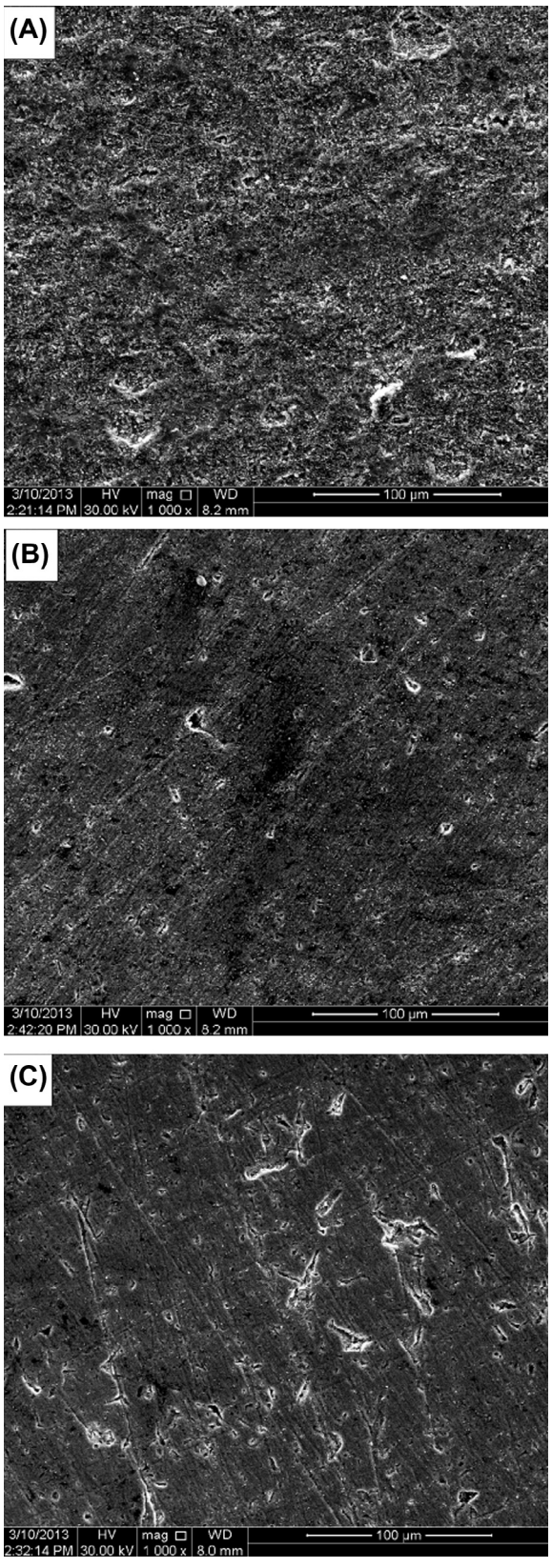

Figure 3 SEM images of SS samples after 12 h immersion in 0.5 M H_2SO_4 (A) and in the presence of 1×10^{-3} M inhibitor at room temperature; DPy (B) and TPy (C).

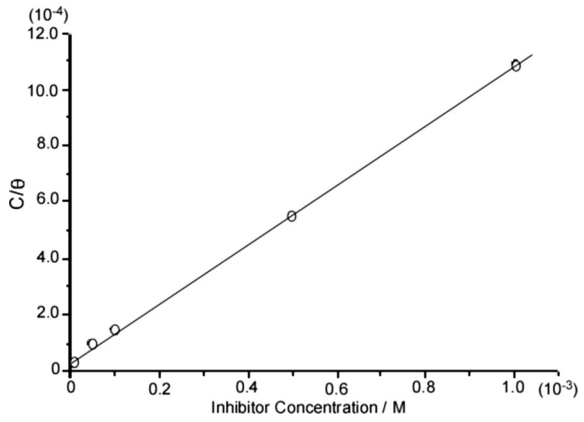

Figure 4 Langmuir isotherm for monolayer TPy inhibitor chemisorptions.

$$\frac{C}{\theta} = \left(\frac{1}{K}\right) + C \tag{5}$$

K is the equilibrium constant of the adsorption process. Plotting of C/θ against C gives a straight line with linear regression coefficient 1.0 ± 0.001 and slope one value for the two inhibitors; Fig. 4 shows the plot of TPy. The calculated K values are 1.05×10^4 and 7.5×10^3 for DPy and 3.44×10^4 and 2.30×10^4 for TPy from polarization and weight loss methods, respectively. There is good agreement between the two methods for the K value which indicated the higher adsorption of the TPy compound on the electrode surface.

The constant K is related to the standard free energy of adsorption ΔG°_{ads} by the equation:

$$K = \left(\frac{1}{55.5}\right)\exp^{\left(\frac{-\Delta G^{\circ}_{ads}}{RT}\right)} \tag{6}$$

where R is the gas constant and T is the absolute temperature. For the investigated inhibitors, ΔG°_{ads} values are −33.44 and −32.6 for DPy, and −36.43 and −35.42 kJ mol^{-1} for TPy, from polarization and weight loss methods, respectively. Generally, the electrostatic interaction between the charged molecules and the charged metal surface (physisorption) is characterized by values of ΔG°_{ads} around −20 kJ/mol or lower while the charge sharing or charge transfer from the organic molecules to the metal surface to form a coordinate type bond (chemisorption) is characterized by values of ΔG°_{ads} around −40 kJ/mol or higher (Lebrini et al., 2007). This result indicates that the inhibitors under study are adsorbed chemically on the steel surface.

3.5. Effect of temperature

The effects of temperature on the inhibitive action of the studied inhibitors were performed. The polarization electrochemical measurements of the SS were carried out in 0.5 M H_2SO_4 and in the absence and presence of 1×10^{-3} M inhibitor at different temperatures (25–40 °C), and the results are recorded in Table 4. As expected the corrosion current increased with an increase in temperature; however the IE of both used inhibitors increased with temperature, indicating that the adsorption process of the inhibitors on the SS surface is endothermic. The SE of the two inhibitors did not largely change with temperature. These results reflect a strong adsorption of the studied compounds on the steel surface.

The dependence of corrosion current on the temperature can be expressed with Arrhenius equation:

$$\log i_{corr} = \log \lambda - \left(\frac{E_a}{2.303RT}\right) \tag{7}$$

where λ is the pre-exponential factor and E_a is the apparent activation energy of the corrosion process. Plotting of log i_{cor} vs. $1/T$ produced a straight line as shown in Fig. 5. Values of E_a for SS in H_2SO_4 in the absence and presence of 1×10^{-3} M inhibitor were determined from the produced lines. The values of E_a in the pure solution and in the presence of DPy and TPy are 137.8, 39.6 and 96.1 kJ mol^{-1}, respectively. The lower values of E_a in the presence of the inhibitors and the general increase of their IE with increasing temperatures are indicative of chemisorption (interaction of unshared electron pairs in the adsorbed molecule with the metal) of these compounds on the steel surface.

3.6. Quantum chemical calculations

Quantum chemical calculations were performed to explain the relationship between the molecular structure and the inhibitive action of the inhibitors under study. Fig. 6 presents quantum

Table 4 Effect of temperature on the corrosion parameters of SS.

Medium (M)	Temperature (°C)	$-E_{cor}$ (mV)	I_{cor} (mA cm^{-2})	b_a (mV decade^{-1})	b_c (mV decade^{-1})	IE (%)	$-E_{pp}$ (mV)	I_{crit} (mA cm^{-2})	SE (%)
0.5 M H_2SO_4	25	497	0.88	52	163		392	27.5	
	30	495	3.43	69	164		388	35.5	
	35	482	6.15	92	179		403	28.5	
	40	496	13.1	112	178		396	63.1	
	25	439	0.41	47	173	53.4	356	16.2	41.1
+ Dpy (1×10^{-3})	30	449	0.48	34	165	86.0	378	19.0	46.5
	35	464	0.59	32	165	90.4	387	17.6	38.2
	40	473	0.89	35	182	93.2	376	31.3	50.4
	25	456	0.125	35	147	85.8	377	18.9	31.3
+ TPy (1×10^{-3})	30	438	0.28	21	149	91.8	378	11.8	66.8
	35	474	0.36	40	168	94.2	386	11.7	58.9
	40	473	0.89	35	182	93.2	376	22.3	64.7

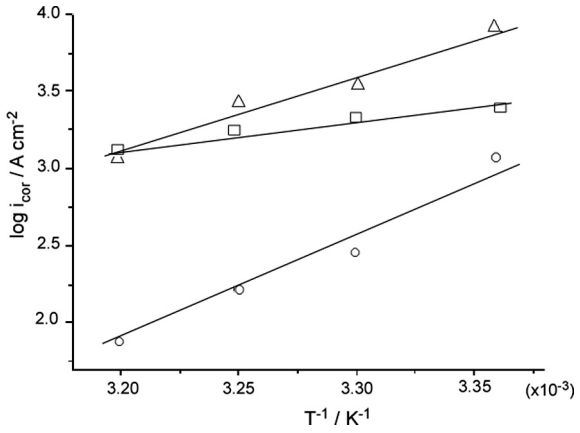

Figure 5 Arrhenius plots for SS in H_2SO_4 in the absence (○) and presence of 1×10^{-3} M inhibitor; DPy (□) and TPy (Δ).

chemical parameters computed for the studied inhibitors, namely energies of the highest occupied molecular orbital (HOMO), the lowest unoccupied molecular orbital (LUMO) and the energy gap ($\Delta E = E_{LUMO} - E_{HOMO}$). Fig. 6 also presents the electrostatic potential map, the total optimized energy, and the dipole moment of the two inhibitors. As shown in Fig. 6, the HOMO in DPy is localized mainly around the π-framework. In contrast, the HOMO in TPy is localized largely on nitrogen atoms and around the aromatic system, which enhances electron donation from the TPy inhibitor to the metal surface. The data in Fig. 6 reveal that TPy has higher values for both E_{HOMO} and E_{LUMO} and a small ΔE (1.5 eV) value. The corresponding value of the energy gap (ΔE) for DPy is 5.5 eV. In principle a decrease in the energy gap leads to easier polarization of the molecule and greater adsorption on the surface (Fouda and Ellithy, 2009). Thus, a small ΔE in TPy facilitates adsorption, and enhances the efficiency of inhibition.

The charge distribution in a molecule can provide critical insight into its physical and chemical properties. The map of the studied inhibitors is displayed in Fig. 7. The electrostatic potential map indicates the size and shape as well as charge distribution of the studied compound. The results from DFT calculations show that TPy has a more negative charge (red color) than DPy. Additionally, the planarity of TPy is more pronounced than DPy. These data clearly show that the negative charge density localized on N atoms and the center aromatic system in TPy is much greater than that in the other inhibitor, indicating that N atoms and π-aromatic are the negative charge centers that donate electrons to the metal in the steel to form a coordinate bond and π-metal interactions, respectively. The dipole moment values support this conclusion. We suggest that the higher value of the dipole moment for TPy (1.7 D) leads to an increase in inhibition, which could be related to the dipole–dipole interaction of molecules and metal surface. Fig. 6 shows a higher dipole moment for TPy in comparison to that of DPy inhibitor. These results explain the good adsorption on the steel surface and, thus, the inhibition efficiency for these compounds and particularly for TPy compared with that of the DPy inhibitor. These theoretical calculations are in good agreement with the experimental results.

3.7. Inhibition process

In this Study, electrostatic adsorption is mostly the first stage of inhibition process which occurred between the cationic species (pyridinium ions) and the negative charged metal surface (Abd El-Maksoud, 2004). The orientation of the adsorbed organic molecules at the metal surface is significant. It has been reported that the surfactant molecules adsorb by its hydrophilic head directing its hydrophobic tail to the solution side (Zyauya and Dawson, 1994). But, the adsorption of the heterocyclic compounds occurs with the aromatic rings sometimes parallel to the metal surface. In case of the pyridinium

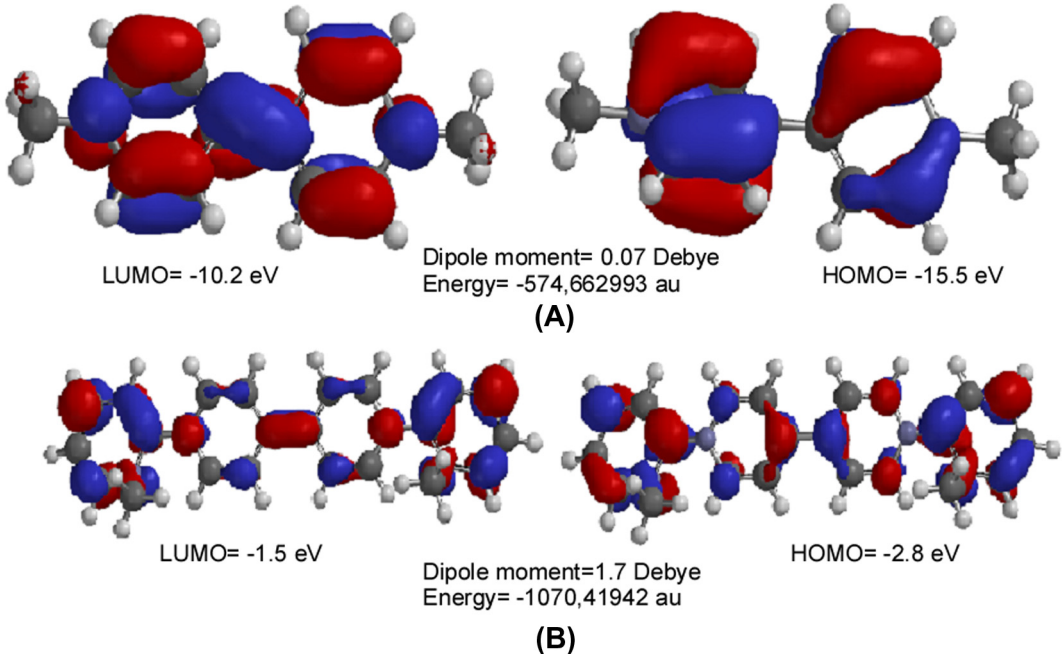

Figure 6 Frontier molecular orbital of the inhibitors.

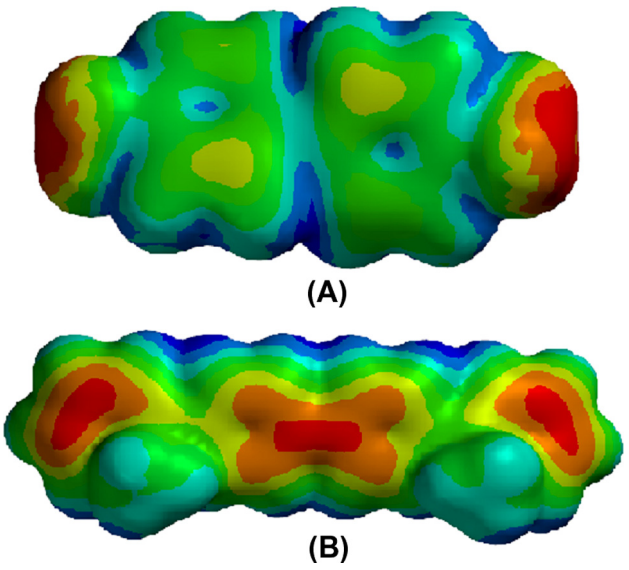

Figure 7 Electrostatic potential map of the inhibitors (red = negative charge and blue = positive charge).

compounds, Saleh explained that the pyridinium ring is in position parallel to the metal surface (Saleh, 2006). It is suggested that the molecules of multi-pyridinium rings are physically adsorbed via the positively charged nitrogen atoms and the aromatic rings are parallel to the surface and the methyl group tail is extended in the solution (Obaid et al., 2013). Thus the tetrapyridinium (TPy) molecule will cover a larger area of metal surface than that of the dipyridinium (DPy) molecule. This is evident by larger inhibition efficiency of the first compound particularly at the lower inhibitor concentration (partially covered of the electrode surface).

The parallel position of the pyridine rings to the metal surface allows for transfer of the π-electrons of these rings to the empty d-orbital of the metal to form coordinate type of link. The chemisorption of TPy and DPy compounds is evident from the increase in inhibition efficiency with temperature, the lower value of E_a and the larger negative value of ΔG°_{ads} in the presence of the inhibitor compound. The DFT calculation confirmed the higher electronic donation and thus interaction for the molecules of these compounds with the metal surface, and the TPy molecules have more ability for chemisorption than that of DPy molecules.

4. Conclusions

(1) The results obtained in this study indicated the effectiveness of the investigated compounds, DPy and TPy, as inhibitors for the corrosion of type 430 SS in aerated sulfuric acid solution.
(2) The compounds work as mixed type inhibitors and enhance the passivation of the SS, and their inhibition efficiencies increase with inhibitor concentration and temperature.
(3) The compounds adsorb chemically on the steel surface and the TPy shows greater inhibition efficiency than that of DPy.
(4) The presence of two additional pyridinium rings attached to the nitrogen atoms in the dipyridinium compound increases the adsorption on the steel surface.

Acknowledgments

This project was funded by the Deanship of Scientific Research (DSR), King Abdulaziz University, Jeddah, under Grant No. (314/130/1431). The authors, therefore, acknowledge with thanks DSR technical and financial support.

References

Abd El-Maksoud, S.A., 2004. J. Electroanal. Chem. 565, 321–328.
Abdel-Aal, M.S., Makhlof, M.Th., Hermas, A.A., 1990. In: Proceedings of the Seventh European Symposium on Corrosion Inhibitor, Ann. Univ. Ferrara, N.S. sezV, Suppl. 9, pp. 1143–1155.
Al-Mayouf, A.M., Al-Suhybani, A.A., Al-Ameery, A.K., 1998. Desalination 116, 25–33.
Aziz, S.A., Obaid, A.Y., Alyoubi, A.O., Abdel Fattah, A.A., 1997. Corros. Prev. Contr. (Dec), 179–182.
Bentiss, F., Lagrenee, M., Trainsel, M., Hornez, J.C., 1999. Corros. Sci. 41, 789–803.
El Achouri, M., Infante, M.R., Izquierdo, F., Kertit, S., Gouttaya, H.M., Nciri, B., 2001a. Corros. Sci. 43, 19–35.
El Achouri, M., Kertit, S., Gouttaya, H.M., Nciri, B., Bensouda, Y.L., Perez, L., Infante, M.R., Elkacemi, K., 2001b. Prog. Org. Coat. 43, 267–273.
Emara, M., 1991. Oriental J. Chem. 7, 78–86.
Fouda, S.A., Ellithy, A.S., 2009. Corros. Sci. 51, 868–875.
Gece, G., Bilgiç, S., 2010. Corros. Sci. 52, 3435–3443.
Hermas, A.A., Morad, M.S., Wahdan, M.H., 2004. J. Appl. Electrochem. 34, 95–102.
Lebrini, M., Lagrenee, M., Vezin, H., Traisnel, M., Bentiss, F., 2007. Corros. Sci. 49, 2254–2269.
Lee, C., Yang, W., Parr, R.G., 1988. Phys. Rev. B37, 785–789.
Li, X., Deng, S., Fu, H., 2011. Corro. Sci. 53, 1529–1536.
Migahed, M.A., 2005. Mater. Chem. Phys. 93, 48–53.
Morad, M.S., Hermas, A.A., Obaid, A.Y., Qusti, A.H., 2008. J. Appl. Electrochem. 38, 1301–1311.
Noor, E.A., 2009. Mater. Chem. Phys. 114, 533–541.
Obaid, A.Y., Al-Thabaiti, S.A., Qusti, A.H., Hermas, A.A., 2013. Asain J. Chem. 25, 3781–3788.
Obot, I.B., Obi-Egbedi, N.O., Umoren, S.A., 2009. Corros. Sci. 51, 276.
Ock, J-Y., Shin, H-K., Kwon, Y-S., Miyake, J., 2005. Colloids Surf. A: Physicochem. Eng. Aspects. 257–258, 351–355.
Özcan, M., 2008. J. Solid State Electrochem. 12, 1653–1661.
Popova, A., Christov, M., Vasilev, A., 2007a. Corros. Sci. 49, 3276–3289.
Popova, A., Christov, M., Vasilev, A., 2007b. Corros. Sci. 49, 3290–3302.
Saleh, M.M., 2006. Mater. Chem. Phys. 98, 83–89.
Spartan, 06 Wavefunction, Inc. Irvine, CA Shao, Y., Molnar, L.F., Jung, Y., Kussmann, J., Ochsenfeld, C., Brown, S.T., Gilbert, A.T.B., Slipehenko, L.V., Levehenko, S.V., O'Neill, D.P., DiStasio Jr., R.A., Lochan, R.C., Wang, T., Beran, G.J.O., Besley, N.A., Herbert, J.M., Lin, C.Y., Van Voorhis, T., Chien, S.H., Sodt, A., Steele, R.P., Rassolov, V.A., Maslen, P.E., Korambath, P.P., Adamson, R.D., Austin, B., Baker, J., Byrd, E.F.C., Dachsel, H.,

Doerksen, Dreuw, A., Dunietz, B.D., Dutoi, A.D., Furlani, T.R., Gwaltney, S.R., Heyden, A., Hirata, S., Hsu, C.P., Kedziora, G., Khalliulin, R.Z., Klunzinger, P., Lee, A.M., Lee, M.S., Liang, W.Z., Lotan, I., Nair, N., Peters, B., Proynov, E.I., Pieniazek, P.A., Rhee, Y.M., Ritchie, J., Rosta, E., Sherrill, C.D., Simmonett, A.C., Subotnik, J.E., Woodcock III, H.L., Zhang, W., Bell, A.T., Chakraborty, A.K., Chipman, D.M., Keil, F.J., Warshel, A., Hehre, W.J., Schaefer, H.F., Kong, J., Krylov, A.I., Gill, P.M.W., Head-Gordon, M., . Phys. Chem. Chem. Phys. 8, 3172.

Stipa, P., 2006. Spectrochim. Acta Part A 64, 653–659.

Wahdan, M.H., Hermas, A.A., Morad, M.S., 2002. Mater. Chem. Phys. 76, 111–118.

Zhang, D.Q., Cai, Q.R., Gao, L.X., Lee, K.Y., 2008. Corros. Sci. 50, 3615–3621.

Zyauya, R., Dawson, J.L., 1994. J. Appl. Electrochem. 24, 943–950.